NVH robust optimization of gear macro and microgeometries using an efficient tooth contact model

Pierre Garambois, Joël Perret-Liaudet, Emmanuel Rigaud

HAL Id: hal-02068279

https://hal.science/hal-02068279

Submitted on 15 Mar 2019

NVH robust optimization of gear macro and microgeometries using an efficient tooth contact model

Pierre Garambois

Post-doctoral researcher

Laboratoire de Tribologie et Dynamique

des Systèmes, UMR CNRS 5513

Ecole Centrale de Lyon

36 avenue Guy de Collongue

69134 Ecully Cedex, France

Email: pierre.garambois@ec-lyon.fr

Emmanuel Rigaud

Associate Professor

Laboratoire de Tribologie et Dynamique

des Systèmes, UMR CNRS 5513

Ecole Centrale de Lyon

36 avenue Guy de Collongue

69134 Ecully Cedex, France

Email: emmanuel.rigaud@ec-lyon.fr

Joel Perret-Liaudet

Associate Professor

Laboratoire de Tribologie et Dynamique

des Systèmes, UMR CNRS 5513

Ecole Centrale de Lyon

36 avenue Guy de Collongue

69134 Ecully Cedex, France

Email: joel.perret-liaudet@ec-lyon.fr

This paper presents a methodology for the multi-objective optimization of both gear macro and microgeometry parameters in order to minimize the Static Transmission Error (STE) and the mesh stiffness fluctuations generated by the meshing process. The optimization is performed using a genetic algorithm which allows testing of a high number of gears. As the repetitive calculation process requires a fast evaluation of the gear excitation sources, a semi-analytical tooth bending model is proposed in order to evaluate gear compliance from a thick Reissner-Mindlin analytical plate model for the evaluation of the tooth strain energy and from a Ritz-Galerkin approximation for the description of the tooth deflection form. For each gear design tested by the algorithm, the robustness of solution to manufacturing errors is evaluated by performing Monte Carlo simulations for a thousand samples of random manufacturing errors. The Probability Density Functions (PDF) describing the RMS values of the mesh stiffness and STE fluctuations of each gear are estimated and their average values are the two objectives minimized by the optimization procedure. Standard deviations and maximum values describing the dispersion of results are also evaluated. Finally, the methodology provides a decision help tool for the designer who intends to choose the best gear design according to the criteria retained. The method is illustrated for a mechanical system equipped with a reverse gear.

Nomenclature

a'	Center distance
b	Gear facewidth
C	Gear torque
C_β	Parabolic and symmetrical gear crowning
$\mathbf{e}(\theta)$	Vector describing the initial gap between the teeth at the angular position θ
E	Young Modulus
f	Rotating frequency of the shaft
f_m	Meshing frequency
$f_{H\alpha}$	Gear tip relief
F	Gear load
g_s	Specific glide
$\mathbf{H}(\theta)$	Compliance matrix of the teeth in contact at the angular position θ
$h(x)$	Thickness of the plate at the heigh x (0 being the tooth foot)
h_a	Tooth addendum coefficient
h_e	Tooth height
h_f	Tooth dedendum coefficient
j	Gear backlash
$k(t)$	Gear mesh stiffness
$L_{f_{H\alpha}}$	Gear tip relief length
m_k	Average value of the PDF describing RMS values of $k(t)$ fluctuations
m_{ste}	Average value of the PDF describing RMS values of STE $\delta(t)$ fluctuations
$(M_x, M_y)^T$	Bending moments
$(Q_x, Q_y)^T$	Shear stress forces
M_k	Maximum value of the PDF describing RMS values of $k(t)$ fluctuations
M_{ste}	Maximum value of the PDF describing RMS values of STE $\delta(t)$ fluctuations
M_{xy}	Twisting moments
n_{MC}	Number of Monte Carlo simulations
N	Number of angular positions of the driving wheel in a meshing period
$\mathbf{P}(\theta)$	Load distributed along the gear contact line at the angular position θ
P_i	Load at the discretized contact point i
r_b	Gear base radius

r_f	Gear root radius
r_i	Gear reference radius
$s_R(R)$	Tooth thickness at the radius R
s_i	Tooth thickness at the reference radius r_i
S	Surface of the plate
$T(x_0, y_0)$	Transverse force applied to the point (x_0, y_0)
$\mathbf{u}(x, y)$	Displacement vector of the plate
$w(x, y)$	Deflection of the plate in the direction z in function of (x,y) the position in the tooth
W_{def}	Strain energy of the plate
x_{ps}	Gear profile shift coefficient
Z	Number of teeth
α_o	Gear pressure angle
α_{oT}	Gear transverse pressure angle
β	Gear helix angle
ε	Strain tensor of the plate
$\delta(\theta)$	Static Transmission Error (STE) at the angular position θ
ν	Poisson coefficient
σ_k	Standard of the PDF describing RMS values of $k(t)$ fluctuations
σ_{ste}	Standard of the PDF describing RMS values of STE $\delta(t)$ fluctuations
$\theta_x(x, y)$	Rotation sectio around x of the plate
$\theta_y(x, y)$	Rotation sectio around y of the plate
$\tilde{\sigma}$	Generalized stress of the plate
inv	Involute operation

1 Introduction

Mechanical gear systems involve internal excitations responsible for upsetting vibroacoustic phenomena [1]. It is usually assumed that the Static Transmission Error (STE) $\delta(t)$ is the main excitation source generated by the meshing process. It is defined as the difference between the actual position of the output wheel and the position it would occupy if the gear drive were perfect and infinitely rigid [2, 3]. Its time-evolution depends on the instantaneous situations of the meshing tooth pairs which results from two physical sources. The first source corresponds to the under load gear teeth deflections. The second source correspond to the tooth

flank micro-geometry associated with manufacturing errors and/or profile/longitudinal tooth corrections. The misalignment induced by the global deformation of the device can be included in the second source. STE is an excitation source which can be taken into account by its time-evolution (displacement type excitation) and a mesh stiffness fluctuation $k(t)$, origin of a parametric excitation of the mechanical gear system. Under steady-state operating conditions, STE and mesh stiffness fluctuations are periodic functions. In the absence of pitch errors and eccentricity faults, their fundamental frequency corresponds to the meshing frequency ($f_m = Zf$, with f the rotation frequency of a wheel and Z its number of teeth). Under operating conditions, STE $\delta(t)$ and $k(t)$ lead to dynamic mesh forces which are transmitted to the housing through wheel bodies, shafts and bearings. Housing vibratory state is directly related to the whining noise radiated by the gearbox [4, 3, 5, 6]. Controlling these excitations is an important key for Noise Vibrations and Harshness (NVH) reduction.

The computation of the STE for spur and helical gears from analysis of the static unilateral contact between teeth is well mastered [7, 8, 9]. Initial gap between unloaded contact surfaces is deduced from tooth flank micro-geometry. Gear teeth compliance is usually deduced from a previous finite element modeling of the gear teeth. Contact equations computation leads to the driven wheel displacement relative to the driving pinion one and the load distribution along the contact line. This computation is performed for each successive position of the driving pinion along the meshing process in order to build the STE time-evolution. Furthermore, the mesh stiffness is deduced from the derivative of the STE with respect to the transmitted load F.

The effect of the micro-level geometry on the STE has been widely studied, as well as the influence of the wheel body deflection and the coupling between the teeth in the meshing process [10, 11, 12, 13, 14, 15, 16].

Micro-level corrections may be used to modify the load distribution, the stress and the wear of teeth [17, 18, 19, 20]. These corrections have also been used to minimize STE and mesh stiffness fluctuations and so the noise induced [21,11,13,17,22].The variability of excitations generated by the presence of micro-level manufacturing error has also been studied [23]. These observations bring us to consider NVH optimization of gear geometries.

Various gear optimization have been implemented in the literature. Some of them focus on stress or weight minimization [24, 6, 25, 26, 27, 28], considering macro-level design parameters as factors (mostly module, number of teeth, tooth addendum and dedendum, shift profile [24, 27, 28]). Some others concern minimization of excitation sources, dynamic phenomena and induced emitted noise [7, 29, 6, 30, 31, 22, 32, 33, 34, 5], considering micro-level parameters (mostly longitudinal and profile tooth flank corrections [21,7,29,10,11,13,30,31,18,19,35,36,37,38]). Dedicated algorithms are sometimes developed [24, 33] and metaheuristic algorithms are used [27, 28, 36, 38]. Mono-objective [24, 33, 28] or multi-objective [27] gear optimizations are both performed.

Large varieties of methods are used in the literature to perform Multi-Objective (MO) optimization, such as gradient-method [39, 40], Particle Swarm Optimization (PSO) [34] and MO Evolutionary Algorithms (EA) methods [41, 42] to cite a few. Most of the time, gradient methods are the simplest to use when both the objective and Jacobian functions are defined. On the other hand, MOEA present two major advantages: they can deal with 0-order objective functions and they act on the total design space. In this field, many methods are available [43] such as Strength Pareto Evolutionary Algorithms (SPEA [44, 45] and SPEA-II [46]), Non-dominated Sorting Genetic Algorithms (NSGA [47] and NSGA-II [48, 49]), Pareto Archived Evolution Strategy (PAES [50]) or Adaptive Pareto

Algorithm (APA [51, 52]). These methods give a set of Pareto-optimal solutions. A major inconvenient is the repetition of the criteria's evaluation for each individual which may lead to prohibitive computation (CPU)-time.

The goal of this paper is to present a multi-objective optimization methodology using an evolutionary algorithm that minimizes, in the context of NVH process, the excitation sources generated by the meshing process (STE and mesh stiffness fluctuation). The factors of the optimization procedure are both the gear macro and micro-geometry parameters. The optimization also takes into account the robustness of the obtained solutions to manufacturing errors within tolerance classes. As the number of required gear samples for EA must be very important, a fast and efficient semi-analytical tooth bending model is defined and introduced in order to evaluate the gear excitation sources associated with each gear sample.

In section 2, the semi-analytical tooth bending model is built in order to obtain a fast evaluation of the gear teeth compliance. The model is used to solve the equations describing unilateral contact between gear teeth and compute STE and mesh stiffness fluctuations. Section 3 presents the multi-objective NVH global optimization procedure of the gear macro and micro-geometries using a genetic algorithm. The robustness of each individual/gear tested to the manufacturing errors is also checked using Monte Carlo simulation and a thousand samples of random errors within the tolerance class associated with the manufacturing process. Even though the mesh stiffness depends on the STE, minimizing the one doesn't lead to minimize the other. The two objectives of the optimization are then the following:

- minimizing the average of the PDF describing the RMS values of STE $\delta(t)$ fluctuations estimations,
- minimizing the average of the PDF describing the RMS values of $k(t)$ fluctuations estimations.

Section 4 briefly presents the NSGA-II algorithm method used to perform the optimization. In the last section 5, the method is illustrated with an optimization example.

2 Deterministic computation of the Static Transmission Error and the mesh stiffness fluctuations

In this part, we present the deterministic computational model used in the optimization procedure to evaluate the periodic excitations generated by a gear.

2.1 Analytical tooth bending model

Computation of the Static Transmission Error firstly requires the estimation of the loaded teeth deflection. Most of times, a compliance matrix is built in a prior calculation, from a finite element modeling of the toothed wheels. All of the physical phenomena that participate in the tooth deflection should be taken into account. The influence of the wheel elasticity and the interaction between the adjacent teeth in the meshing process are all the more important that the wheel body is thin [8, 9]. Despite a proven efficiency [8, 9], the built of a finite element meshing and the work on large stiffness matrices are time-consuming. So that, the cost in computing time is prohibitive in the case of the implementation of a robust optimization needing a lot of gear macro-geometries built and tested. In this context, a semi-analytical modeling of the compliance matrix has been developed. It is based on the Reissner-Mindlin thick plate analytical theory [53, 54] described in this part, coupled with a Ritz-Galerkin approximation for the teeth deflection form (see next section 2.2).

The gear tooth is modeled with a rectangular plate with variable thickness $h(x)$ depending on the gear macro-geometry parameters. The deflection of the the plate $w(x, y)$ is used to model the deflection of the tooth. The simplified model is depicted in figure 1 and uses a Reissner-Mindlin thick plate theory (see figure 2). The strain energy W_{def} of a thick plate (surface S) in a plane (x, y) submitted to a force the transverse force $T(x_0, y_0)$

is defined as follows:

$$W_{def} = \iint_S \frac{1}{2}\varepsilon^T \tilde{\sigma}(\varepsilon) - w(x_0,y_0)T(x_0,y_0)\,dS \qquad (1)$$

with ε et $\tilde{\sigma}$ respectively the strain and generalized stress of the plate.

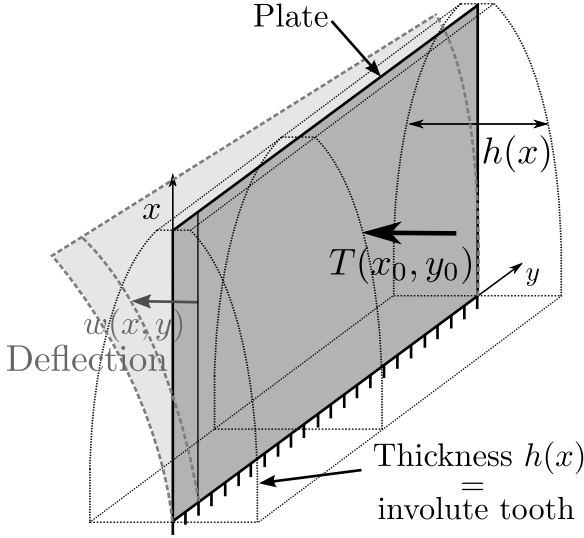The displacement vector $\mathbf{u}(x,y)$ is defined as follows:

Fig. 1: *Analytical tooth bending model*

$$\mathbf{u}(x,y) = \begin{Bmatrix} w(x,y) \\ \theta_x(x,y) \\ \theta_y(x,y) \end{Bmatrix} \qquad (2)$$

with $w(x,y)$, $\theta_x(x,y)$ and $\theta_y(x,y)$ respectively the deflection of the plate, the rotation of section around x and y at the point (x,y). The strain ε and generalized stress $\tilde{\sigma}$ at a point (x,y) are defined by:

$$\varepsilon = \begin{Bmatrix} \varepsilon_{xx} \\ \varepsilon_{yy} \\ \gamma_{xy} = 2\varepsilon_{xy} \\ \gamma_{xz} = 2\varepsilon_{xz} \\ \gamma_{yz} = 2\varepsilon_{yz} \end{Bmatrix} = \begin{Bmatrix} \frac{\partial \theta_y}{\partial x} \\ -\frac{\partial \theta_x}{\partial y} \\ \frac{\partial \theta_y}{\partial y} - \frac{\partial \theta_x}{\partial x} \\ \theta_y + \frac{\partial w}{\partial x} \\ -\theta_x + \frac{\partial w}{\partial y} \end{Bmatrix} \qquad (3)$$

$$\tilde{\sigma}(\varepsilon) = \begin{Bmatrix} M_{xx} \\ M_{yy} \\ M_{xy} \\ Q_x \\ Q_y \end{Bmatrix}$$

$$= \frac{E}{1-\nu^2} \begin{Bmatrix} \frac{h^3}{12} & \nu\frac{h^3}{12} & 0 & 0 & 0 \\ -\nu\frac{h^3}{12} & \frac{h^3}{12} & 0 & 0 & 0 \\ 0 & 0 & \frac{(1-\nu)}{2}\frac{h^3}{12} & 0 & 0 \\ 0 & 0 & 0 & \frac{5(1-\nu)h}{12} & 0 \\ 0 & 0 & 0 & 0 & \frac{5(1-\nu)h}{12} \end{Bmatrix} \begin{Bmatrix} \varepsilon_{xx} \\ \varepsilon_{yy} \\ \gamma_{xy} \\ \gamma_{xz} \\ \gamma_{yz} \end{Bmatrix}$$
$$(4)$$

with E the Young modulus and ν the Poisson coefficient. The plate representing the tooth is assumed clamped at the root radius r_f. The thickness $h(x)$ of the plate is equal to the tooth thickness $s_R(R)$ at the radius $R = r_f + x$:

$$s_R(R) = R\left[\frac{s_i}{r_i} - 2\left[\mathrm{inv}(\arccos(\frac{r_b}{R}))] - \mathrm{inv}(\alpha_{oT}))\right]\right] \qquad (5)$$

with

$$s_i = m_o\left[\frac{\Pi}{2} + 2x_{ps}\tan(\alpha_o)\right] \qquad (6)$$

and m_o the gear module, α_o the normal pressure angle, x_{ps} the profile shift coefficient, r_i the reference radius, r_b the base radius and α_{oT} the transverse pressure angle. "Inv" is the involute function corresponding to:

$$\mathrm{inv}(\alpha) = \tan(\alpha) - \alpha \qquad (7)$$

2.2 A Ritz-Galerkin approximation

A Ritz-Galerkin polynomial interpolation is made to approximate the 3 displacement fields over the plate. These ones are described using chosen kinematically admissible functions respecting the following conditions:

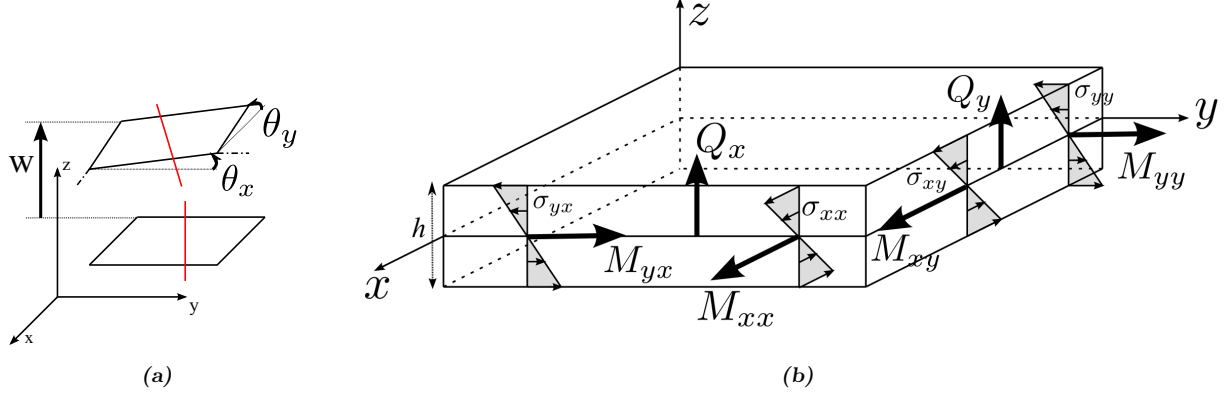$$\begin{cases} w(0,y) = 0 \\ \theta_x(0,y) = 0 \\ \theta_y(0,y) = 0 \end{cases} \qquad (8)$$

Fig. 2: *Reissner-Mindlin theory: (a) Displacements, (b) Generalized stress: bending moments $(M_x, M_y)^T$, twisting moment M_{xy} and shear stress forces $(Q_x, Q_y)^T$*

The displacements of a given point (x, y) are written as follows:

$$\mathbf{u}(x,y) = \begin{Bmatrix} w(x,y) \\ \theta_x(x,y) \\ \theta_y(x,y) \end{Bmatrix} = \begin{Bmatrix} x(a_w + b_w y + c_w x) \\ x(a_{\theta_x} + b_{\theta_x} y + c_{\theta_x} x) \\ x(a_{\theta_y} + b_{\theta_y} y + c_{\theta_y} x) \end{Bmatrix} \quad (9)$$

with a_w, b_w, c_w, a_{θ_x}, b_{θ_x}, c_{θ_x}, a_{θ_y}, b_{θ_y} and c_{θ_y} the 9 coefficients that define the 3 fields $w(x,y)$, $\theta_x(x,y)$ and $\theta_y(x,y)$ of the displacement vector $\mathbf{u}(x,y)$.

The 9 unknowns parameters of the Ritz-Galerkin approximation 9 are identified from application of the minimum total potential energy principle to equation 1. A symbolic scientific computing software was used in order to obtain the 3 fields $w(x,y)$, $\theta_x(x,y)$ and $\theta_y(x,y)$ of the displacement vector $\mathbf{u}(x,y)$. These analytical expressions are function of:

- the gear macro-geometry parameters governing the tooth thickness $h(x)$,
- the material characteristics (E and ν),
- the position (x_0, y_0) and intensity of the force T,
- the position (x, y) of the point where the deflection $w(x,y)$ and the rotations of section $\theta_x(x,y)$ and $\theta_y(x,y)$) are evaluated.

The accuracy of the analytical thick plate model coupled with the Ritz approximation has been compared to a finite element model. A MAC-like criterion was used to compare the plate deflection forms obtained with our semi-analytical model and a classical plate finite element model. It shows a good correlation with an 95% accuracy.

For each individual/gear tested in the genetic algorithm, the semi-analytical tooth bending model allows the computation of the compliance matrices (for each angular position θ in the meshing period) from the gear macro-geometry in less than 1 second using MATLAB software coupled with an Intel Core i7-5500U processor (2.40 GHz, 2 core) and RAM 16 Go. More than 1000 seconds are necessary when the meshing of gear teeth are required with a finite element modeling.

2.3 Static Transmission Error STE $\delta(t)$ and mesh stiffness fluctuations $k(t)$

For a given transmitted load F, Static Transmission Error (STE) $\delta(t)$ is calculated for a set of successive positions θ of the driving wheel, in order to evaluate its periodic time evolution. For each angular position θ of the driving wheel, a kinematic analysis of gear mesh allows the location of theoretical contact lines for each loaded tooth pair. The contact lines are discretized in segments where the force is assumed constant. A compliance matrix $\mathbf{H}(\theta)$ of the contact lines at the wheel position θ is then introduced, and links the displacements of the discrete points to the applied forces. This

matrix is built using the semi-analytical tooth bending model described in the two last sections 2.1 and 2.2. The Hertz deformation is added in the compliance matrix $\mathbf{H}(\theta)$. On each segment of the discretized contact lines, an initial gap distance needs to be taken into account. This gap, represented by the vector $\mathbf{e}(\theta)$, is induced by the tooth flank corrections, the manufacturing errors and the parallelism errors which result from the elasto-static deformation of the gearbox. For each position θ over a meshing period, the contact equation can be written as follows:

$$\begin{cases} \mathbf{H}(\theta).\mathbf{P}(\theta) = \delta(\theta).\mathbf{1} - \mathbf{e}(\theta) \\ \mathbf{1}^T.\mathbf{P}(\theta) = F \end{cases} \quad (10)$$

under the following constraints:

$$\begin{cases} \mathbf{H}(\theta).\mathbf{P}(\theta) + \delta(\theta).\mathbf{1} \geqslant \mathbf{e}(\theta) \\ P_i \geqslant 0 \end{cases} \quad (11)$$

where the unknowns are the STE $\delta(\theta)$ and the load $\mathbf{P}(\theta)$ distributed along the contact lines.

For each of the successive positions θ of the driving wheel, the mesh stiffness is defined as the derivative of STE relative to the transmitted load F:

$$k(\theta) = \frac{\partial F}{\partial \delta(\theta)} \quad (12)$$

The mesh stiffness is evaluated for the set of successive positions θ of the driving wheel, in order to evaluate its periodic time evolution. Practically, it is estimated by numerical derivation rule.
Figure 3 displays the excitation sources generated by the meshing process.

Figure 4 displays the Static Transmission Error and mesh stiffness fluctuations for two sets of macro and micro-geometry parameters presented in the table 1. Results obtained with a compliance matrix computed with the analytical tooth bending model are compared with results obtained from a finite element modeling of
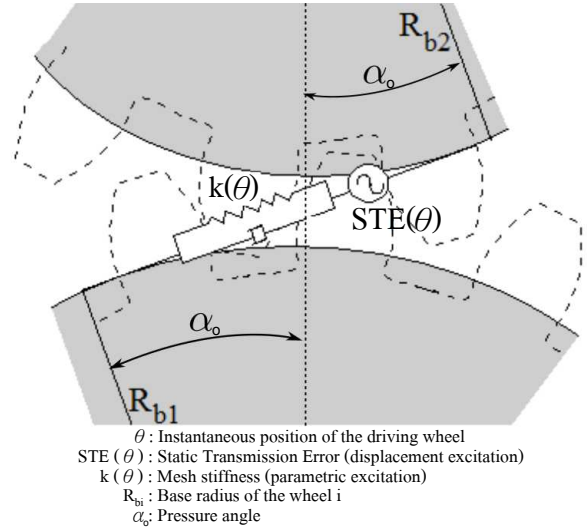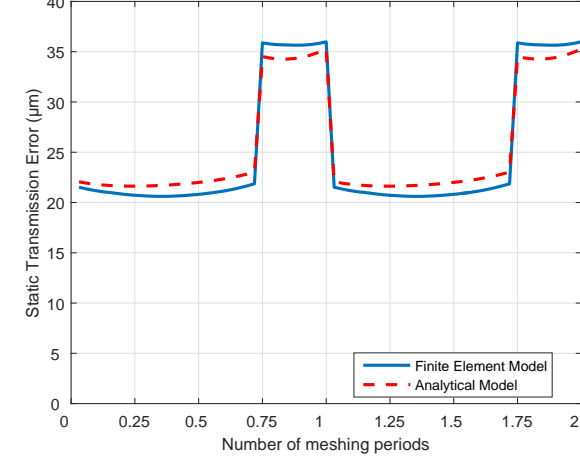

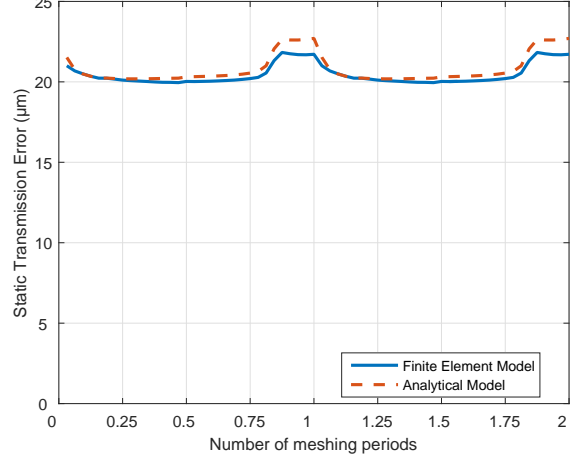**Fig. 3:** *Excitation sources generated by the meshing process [55]*

the gear teeth. The results demonstrate the good accuracy of the analytical tooth bending model. Many additional comparisons performed with various macrogeometries in terms of module, number of teeth, helix, pressure angles and torques transmitted have shown a relative error which remains under 10%, for both the mean and peak-to-peak values of static transmission error and mesh stiffness. Only some anecdotal cases may show a relative error upt to 25%.

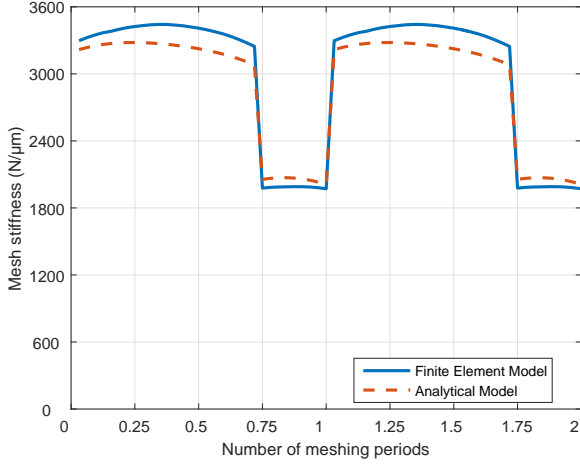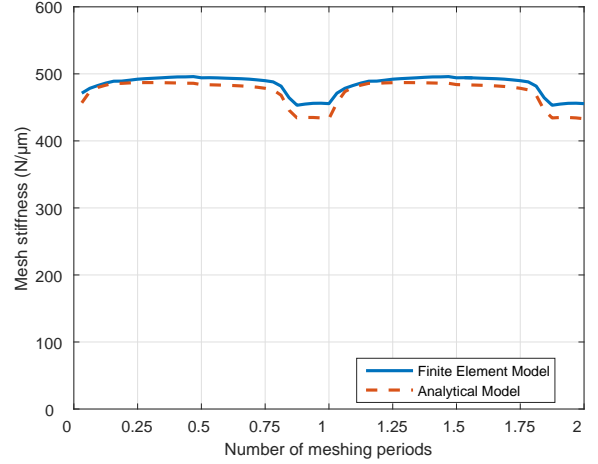| Case	1	2
Young Modulus E (GPa)	210	
Poisson coefficient ν	0.3	
Number of teeth Z (wheel 1/2)	33/75	17/71
Module m_o (mm)	12	2.676
Pressure angle α_o (degrees)	20	20
Facewidth b (mm)	90	20
Helix angle β (degrees)	0	25.648
Addendum coefficient h_a (wheel 1/2)	0.99/0.99	1.15/1.13
Dedendum coefficient h_f (wheel 1/2)	1.25/1.25	1.65/1.62
Center distance a' (mm)	650	128
Torque on the wheel 1 (N.m)	13200	230

Table 1: *Gears tested*

Fig. 4: *Periodic evolution of STE and mesh stiffness over two meshing period for 2 different gears: comparison between Finite Element Model and Analytical Model. (a) STE $\delta(t)$ of gear 1. (b) STE $\delta(t)$ of gear 2. (c) $k(t)$ of gear 1. (d) $k(t)$ of gear 2.*

3 Optimization problem

The NVH (Noise, Vibration and Harshness) multi-objective optimization aims to find the gear macro and micro-geometry parameters that minimize the excitations generated by the meshing process under the operating conditions, respecting wear conditions, and taking into account the robustness of the solutions to the manufacturing errors.

3.1 Robust objectives

STE and mesh stiffness fluctuations are highly depending on the manufacturing and assembly errors [23] (which are taken into account through the vector $\mathbf{e}(\theta)$ of the equation 10). Solution of the optimization procedure should take in account the parameters variability. For each gear tested by the algorithm, a precision corresponding to the tolerance class 6 (ISO 1328) is assumed. The manufacturing errors taken into account are the following:

- profile errors (linear and parabolic),
- longitudinal errors (linear and parabolic),
- parallelism errors (axis inclination and deviation).

The manufacturing errors distribution is considered to be uniform over the range associated with the tolerance class, which is the worst possible case in. In order to consider the variability of the results induced by such tolerances, the objectives considered are statistical averages. A Monte-Carlo simulation is performed for each gear with $n_{MC} = 1000$ random manufacturing error samples and the Probability Density Functions (PDF) describing the RMS values of STE $\delta(t)$ and mesh stiffness $k(t)$ fluctuations are built (see an example in figure 5). The choice of $n_{MC} = 1000$ combines both a good accuracy (around 3%) and a reasonable CPU-time. The objectives of the optimization are the following:

- minimizing the average value m_{ste} of the PDF describing the RMS values of STE $\delta(t)$ fluctuations estimations,

$$m_{ste} = \sum_{i=1}^{n_{MC}} \frac{\text{RMS}\left[\delta_i(t) - \overline{\delta_i(t)}\right]}{n_{MC}} \qquad (13)$$

- minimizing the average value m_k of the PDF describing the RMS values of $k(t)$ fluctuations estimations.

$$m_k = \sum_{i=1}^{n_{MC}} \frac{\text{RMS}\left[\frac{k_i(t) - \overline{k_i(t)}}{\overline{k_i(t)}}\right]}{n_{MC}} \qquad (14)$$

Other characteristics of the PDF, such as the standard deviation σ and the maximum value M are used in the last section 5.

3.2 Parameters

The parameters of the optimization are both macro and micro geometry parameters, namely:

- the gear cutting tool, that defines the normal module m_o and the normal pressure angle α_o,
- the teeth number Z_1, Z_2,
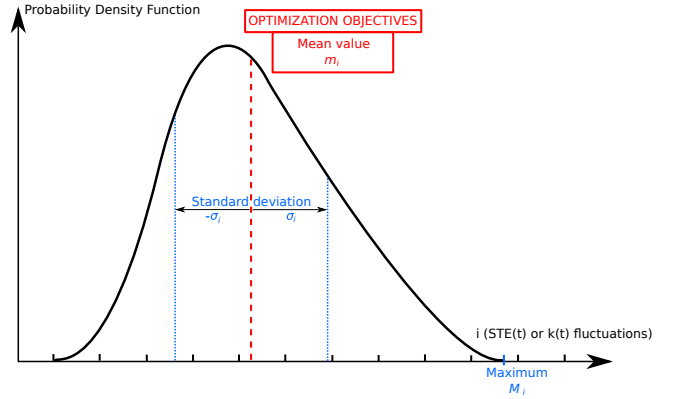- the helix angle β,

Fig. 5: *Power Density Function of signal i (STE $\delta(t)$ or $k(t)$ for one gear tested*

- the tooth addendum h_a,
- the crowning magnitude C_β, corresponding to a micro-geometrical parabolic and symmetrical longitudinal tooth flank correction,
- the tip relief magnitude $f_{H\alpha}$ and the tip relief length $L_{f_{H\alpha}}$ corresponding to a micro-geometrical tooth profile correction.

They are chosen under some constraints, namely:

- the gear ratio is imposed,
- the center distance a' is imposed,
- the gear facewidth b is imposed,
- the gear backlash j is set,
- the material is imposed,
- the tooth dedendum coefficient h_f is set (default value = 1.25),
- the total contact ratio is more than 1.1,
- the specific sliding ratio g_s is less than 2.5,
- the maximum contact pressure and mechanical strength are less than a material dependent limit.

One may note that the profile shift coefficient x_{ps} is deduced from the other parameters, especially the center distance a' and the gear backlash j.

In this way, a gear tested by the algorithm (i.e. an individual) is a combination of a macro and micro-level geometry parameters. For each gear, a Monte Carlo simulation with 1000 random manufacturing errors is
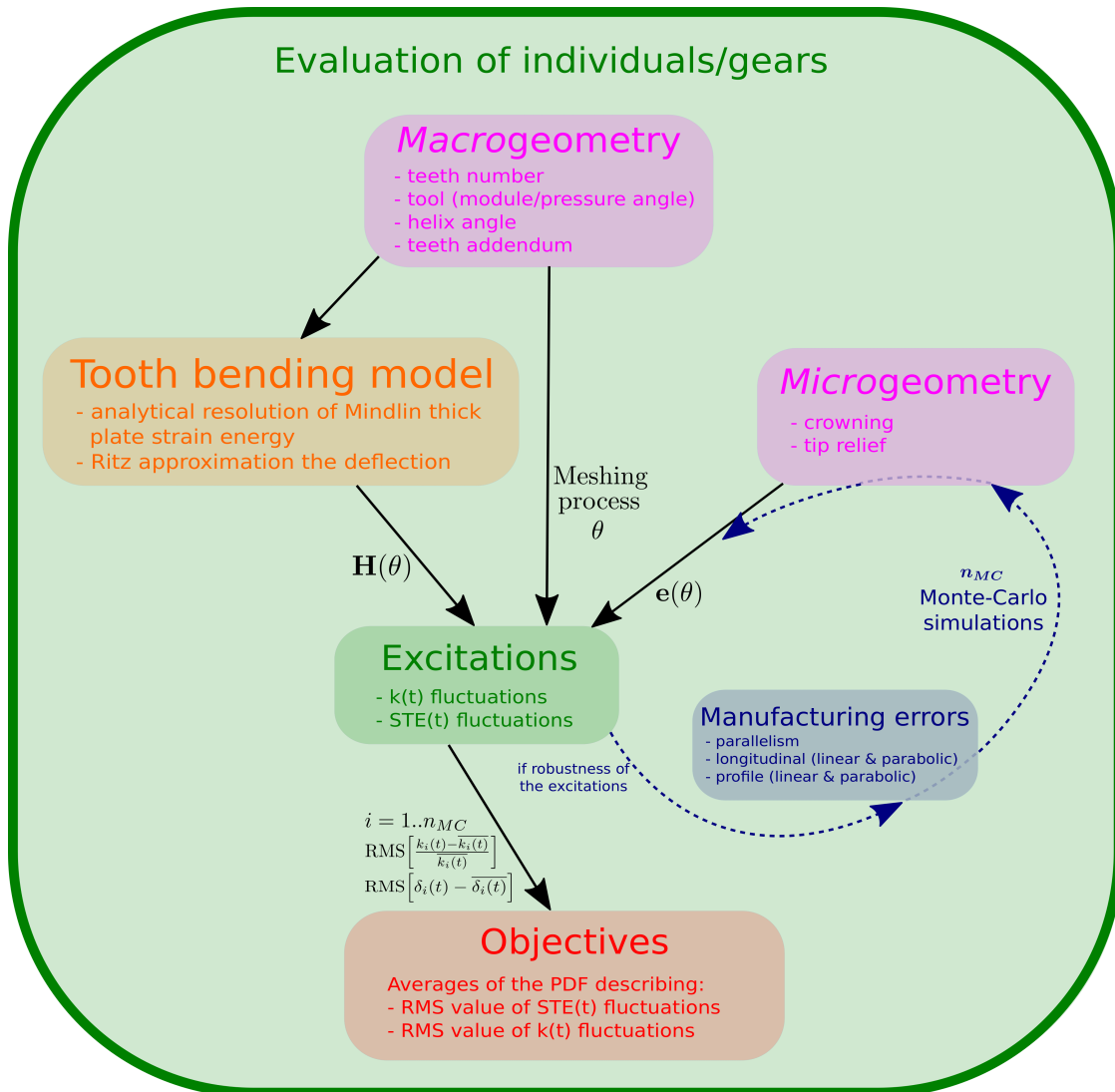
Fig. 6: *Principle of the evaluation of each gear*

made. The objectives are the averages m_{ste} and m_k of the the PDF describing the STE and mesh stiffness fluctuations RMS values. The principle of the evaluation of each individual/gear is described in figure 6.

4 Principle of the genetic algorithm

Genetic algorithm methods are based on the evolution of species over generations in their natural environment. Figure 7 summarizes the principle of such method. The algorithm used is called NSGA-II [48, 49]. "Individuals" are considered. In this paper, each individual corresponds to a gear (which means a combination a macro and micro-geometry parameters) associated with its two objectives (see section 3.1). A group of independent individuals form a "population". The goal of the algorithm is to make the population evolve over the "generations" (iterations) by doing "mutations" and "crossing" between the individual's parameters of this population, in order to improve the objectives of the individuals in the population. The algorithm is composed of 5 different stages (see figure 7). Figure 6 gives a detailed insight of the evaluation step 2.

For populations composed of 100 gears evolving over 200 up to 300 generations, the number of gears tested by the algorithm is larger than 20 000. The results focus on the last generation obtained by the algorithm. Usu-
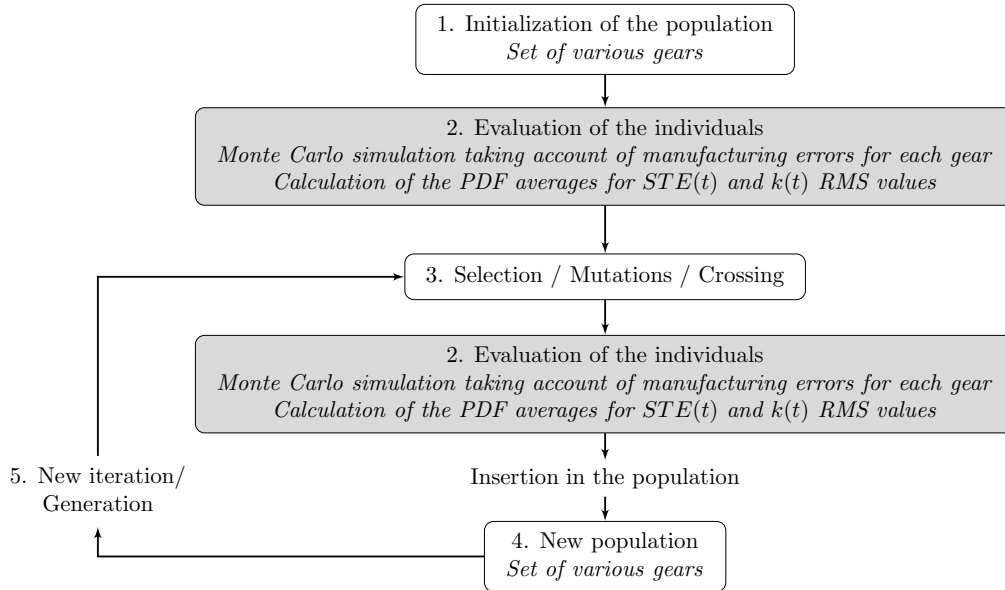
Fig. 7: *Functioning of the genetic algorithm NSGA-II*

ally, this last population is composed of Pareto-optimal solutions, which correspond to gears that are compromises between the two antagonistic objectives. In other words, each solution (gear) of this Pareto front is better than the others in the sense of at least one of the objectives.

5 Application example

5.1 Mechanical gear system studied

An application example is presented in this part in order to demonstrate the efficiency of the overall procedure. It considers a kinematic chain composed of two contra-rotative shafts driven by a reverse gear (1:1 ratio). The center distance is set to $a' = 38$ mm. The torque transmitted by the gear is set to $C = 10$ N.m. The backlash is set to $j = 0$ μm and the facewidth is set to $b = 8$mm. 3 optimizations were performed for 3 different gear cutting tools (modules and pressure angles: $m_1 = 1$ mm, $\alpha_1 = 20°$; $m_2 = 1.5$ mm, $\alpha_2 = 20°$ and $m_3 = 2$ mm, $\alpha_3 = 20°$). For each gear cutting tool, the teeth number parameter Z fulfills the constraints (see section 3.2), the tooth addendum coefficient maximum is 1, the helix angle β range is $[0..25°]$, the crowning magnitude C_β range is $[0..7\mu$m$]$, the tip relief magnitude

$f_{H\alpha}$ range is $[0..5\mu$m$]$ and the tip relief length $L_{f_{H\alpha}}$ range is $[0..\frac{h_e}{2}]$ (with h_e the tooth height). The manufacturing errors correspond to a quality class 6. For each optimization, more than 20 000 gears were tested and the genetic algorithm provides a last generation composed of 100 gears (population size) which are the best compromises between these two objectives, selected over generations. All the results for the last generation of each gear cutting tool are presented in table 2, each line corresponding to a gear.

The first line corresponds to a standard spur gear with a module $m_o = 1$ mm, a pressure angle $\alpha_o = 20°$ and no micro-level corrections. The 3 next parts correspond to the best solutions obtained for the 3 optimizations (one for each gear cutting tool). Many of the hundred gears which compose the last generation have the same macrogeometry and differ only because of their microgeometry parameters. For the sake of simplicity, only the best microgeometry parameters set is kept for each gear (macrogeometry).

The first column indicates the index of the gear solution G. The second column indicates the gear cutting tool parameters (m_o/α_o). The 4 next columns indicate the

Table 2: *Gears selected*

G	Tool Module m_o/ pressure angle α_o (mm/°)	Macro-level geometry Nb. of teeth Z	Profile shift coeff. xps	Helix angle β (°)	Teeth addendum coeff. ha	Micro-level geometry Crowning C_β (μm)	Tip relief/ length $f_{H\alpha}/L_{f_{H\alpha}}$ (μm & mm)	Objectives PDF Average m_k (%)	m_{ste} (μm)	Objectives dispersion Dev. & maximum σ_k (%)	M_k (%)	Dev. & maximum σ_{ste} (μm)	M_{ste} (μm)
SC	1/20	38	0.000	0	1.000	0	0/0.000	18.0	0.48	1.4	21.6	0.09	0.65
1	1/20	37	0.464	5	0.600	5	0/0.000	8.2	1.61	0.9	10.4	0.34	2.87
2	1/20	37	-0.148	15	0.554	0	5/0.180	9.2	1.30	1.6	16.8	0.20	1.95
3	1/20	36	0.815	10	0.679	0	5/0.193	9.6	1.23	1.4	13.7	0.22	1.97
4	1/20	36	0.815	10	0.598	0	5/0.185	10.0	1.76	1.2	14.9	0.25	2.57
5	1/20	37	0.223	10	0.600	0	5/0.185	10.1	1.84	1.4	13.6	0.25	2.73
6	1/20	37	0.223	10	0.680	0	5/0.193	10.3	1.22	1.5	15.3	0.22	1.88
7	1/20	35	-0.293	25	0.916	0	2/0.000	12.8	0.11	3.6	18.7	0.05	0.27
8	1/20	36	-0.151	20	1.000	0	0/0.900	12.9	0.12	3.7	18.8	0.05	0.29
9	1/20	34	0.252	25	1.000	0	5/0.000	15.2	0.13	2.5	19.2	0.07	0.41
10	1.5/20	24	0.724	5	0.628	5	0/1.409	7.5	1.74	1.0	10.6	0.36	2.83
11	1.5/20	26	-0.336	5	0.405	0	0/0.993	7.9	1.58	0.6	11.0	0.34	2.84
12	1.5/20	25	0.123	5	0.610	0	0/0.000	7.9	1.68	0.6	11.5	0.34	2.70
13	1.5/20	24	-0.101	20	0.610	0	5/0.279	8.6	1.43	1.5	13.4	0.22	2.26
14	1.5/20	23	0.474	20	0.705	0	5/0.293	8.7	1.38	1.3	14.7	0.21	2.03
15	1.5/20	23	-0.022	25	0.677	0	5/0.289	8.9	1.09	1.3	14.2	0.19	1.67
16	1.5/20	23	0.905	15	0.710	0	5/0.294	9.2	1.33	1.2	14.2	0.23	1.93
17	1.5/20	22	0.593	25	0.748	0	5/0.300	9.3	1.08	1.4	15.8	0.19	1.64
18	1.5/20	23	0.474	20	0.764	0	5/0.302	9.3	1.12	1.3	17.0	0.21	1.78
19	1.5/20	23	0.905	15	0.647	0	5/0.285	9.6	1.71	1.2	14.2	0.25	2.42
20	1.5/20	24	0.259	15	0.729	0	5/0.297	9.7	1.33	1.5	15.3	0.23	2.08
21	1.5/20	24	0.259	15	0.662	0	5/0.287	9.7	1.80	1.3	14.9	0.25	2.58
22	1.5/20	24	-0.101	20	0.688	0	5/0.291	10.0	0.99	1.3	14.8	0.20	1.58
23	1.5/20	23	-0.022	25	0.741	0	5/0.299	10.3	0.85	1.2	14.0	0.18	1.42
24	1.5/20	23	0.474	20	0.823	0	5/0.311	10.7	0.91	1.1	15.4	0.19	1.47
25	1.5/20	22	0.593	25	0.849	0	5/0.315	11.1	0.80	1.2	16.5	0.18	1.38
26	1.5/20	22	0.593	25	0.899	0	5/0.645	11.1	0.96	1.7	16.7	0.16	1.45
27	1.5/20	22	0.593	25	0.950	0	5/0.660	11.4	0.83	1.6	18.2	0.15	1.37
28	1.5/20	22	0.593	25	1.000	0	5/0.675	11.6	0.71	1.5	17.6	0.14	1.14
29	1.5/20	23	-0.022	25	0.806	0	5/0.617	11.7	1.02	2.0	16.3	0.16	1.52
30	1.5/20	23	-0.022	25	0.871	0	5/0.636	12.1	0.79	1.8	16.3	0.15	1.25
31	1.5/20	24	-0.101	20	0.766	0	5/0.302	12.5	0.68	1.0	16.1	0.19	1.28
32	1.5/20	23	-0.022	25	0.935	0	5/0.656	12.5	0.60	1.6	16.5	0.13	1.06
33	1.5/20	23	-0.022	25	1.000	0	5/0.675	13.1	0.44	1.4	17.1	0.12	0.94
34	1.5/20	24	-0.101	20	1.000	0	5/0.000	14.2	0.17	2.1	18.6	0.09	0.53
35	1.5/20	24	-0.101	20	0.922	0	5/0.652	14.3	0.51	1.5	17.8	0.13	0.97
36	2/20	18	0.543	5	0.674	7	2/0.385	8.0	2.19	0.9	10.2	0.35	3.23
37	2/20	19	-0.036	5	0.590	0	0/0.000	8.3	1.74	0.6	10.0	0.34	2.80
38	2/20	17	0.126	25	0.747	0	5/0.399	8.6	1.48	1.4	13.2	0.23	2.16
39	2/20	18	0.408	10	0.688	5	0/1.938	8.6	1.67	0.8	11.0	0.34	2.90
40	2/20	17	0.126	25	0.797	0	5/0.409	8.9	1.22	1.4	14.9	0.22	1.92
41	2/20	17	0.521	20	0.795	0	5/0.409	9.3	1.44	1.4	15.9	0.23	2.22
42	2/20	16	0.804	25	0.861	0	5/0.422	9.5	1.11	1.2	14.3	0.22	1.83
43	2/20	17	0.521	20	0.744	0	5/0.399	9.6	1.73	1.3	14.0	0.26	2.73
44	2/20	18	-0.075	20	0.636	0	5/0.377	9.6	1.80	1.3	13.6	0.25	2.59
45	2/20	16	0.804	25	0.818	0	4/0.414	9.6	1.23	1.3	15.5	0.22	2.01
46	2/20	17	0.521	20	0.847	0	5/0.419	9.8	1.21	1.3	14.1	0.23	1.89
47	2/20	17	0.126	25	0.848	0	5/0.420	9.8	1.01	1.2	14.6	0.21	1.59
48	2/20	18	-0.075	20	0.709	0	5/0.392	9.8	1.26	1.5	14.3	0.22	1.92
49	2/20	17	0.859	15	0.734	0	5/0.397	10.0	1.62	1.2	13.8	0.26	2.38
50	2/20	17	0.859	15	0.784	0	5/0.407	10.1	1.35	1.2	13.7	0.24	2.00
51	2/20	16	0.804	25	0.903	0	5/0.431	10.5	1.00	1.2	17.9	0.20	1.62
52	2/20	17	0.126	25	0.899	0	5/0.430	11.0	0.84	1.0	14.9	0.20	1.41
53	2/20	16	0.804	25	0.945	0	5/0.439	11.3	0.89	1.0	15.5	0.19	1.55
54	2/20	16	0.804	25	0.987	0	5/0.895	11.7	1.06	1.5	15.8	0.18	1.61
55	2/20	17	0.126	25	0.949	0	5/0.440	12.0	0.71	0.9	14.8	0.18	1.43
56	2/20	17	0.126	25	1.000	0	5/0.900	12.4	0.88	1.6	16.5	0.17	1.40
AV								17.5	1.45				

macrogeometry parameters ($Z/x_{ps}/\beta/h_a$).

The 3 next columns indicate the micro geometry parameters ($C_\beta/f_{H\alpha}/L_{f_{H\alpha}}$).

The 2 next columns indicate the value of the two objectives (average values m_k and m_{ste} of the PDF describing the RMS values of $k(t)$ and STE $\delta(t)$ fluctuations).

The 4 last columns indicate the standard deviations (σ_k and σ_{ste}) and the maximum values (M_k and M_{ste}) of the PDF describing the RMS values of $k(t)$ and STE $\delta(t)$ fluctuations. They give an insight of the dispersion of the results.

Gears are ranked in ascending order of m_k values for each gear cutting tool.

The last line presents m_k and m_{ste} mean values observed for the 60 000 gears tested during the 3 optimization procedures.

5.2 Results of the optimization procedure

Figure 8 displays the three Pareto fronts obtained at the last generation of each gear cutting tool/optimization. In every front, each point is a gear that is better than the others in the sense of at least one of the two objectives m_k (abscissa) and m_{ste} (ordinate). The form of these fronts demonstrate that the two objectives are antagonistic and not independent: the minimization of the STE $\delta(t)$ fluctuations leads to an increase of $k(t)$ fluctuations, and conversely. This figure also shows that none of the 3 gear cutting tools is better than the others.

Figure 9 displays the Pareto front of the third gear cutting tool ($m_3 = 2$ mm, $\alpha_3 = 20^\circ$) as well as an insight of the robustness of each gear composing the front. A square of [$2\sigma_k$ x $2\sigma_{ste}$] surrounds each point and provide an overview of the robustness of the gear. The figure shows a significant dispersion that potentially enlarges the Pareto front and makes it a relevant point in the optimization choice.

Considering dispersion, the decision is made to

slightly improve the optimization procedure regarding our application, and allow the algorithm to keep some gears that are close to the Pareto front, but not technically in (even if they are not better than the other solutions regarding the two objectives m_k and m_{ste}). These additional gears may present good performance in terms of objectives regarding their robustness, as well as an interest in term of geometry, and need to be taken into account in the results analysis. This way, figure 10 displays a "wide" Pareto front for each of the 3 optimizations, obtained at the last generation of the algorithm. Every gear presented in table 2 corresponds to a point in figure 10.

Optimization procedure performed leads to a wide range of results. For the standard gear (corresponding to a module m_o of 1 mm, a pressure angle α_o of 20°, a teeth number Z of 38, standard addendum and dedendum coefficients and no microgeometry corrections), m_k value is equal to 18% and m_{ste} value is equal to 0.48 μm. For the 60 000 gears tested during the 3 optimization procedures, m_k value is between 7.5 and 29.2% (mean value 17.5%) and m_{ste} value is between 0.133 and 23.60 μm (mean value 17.5%). For gears selected in table 2, m_k value is between 7.5 and 15.2% and m_{ste} value is between 0.133 and 2.19 μm. Most of them show m_k and m_{ste} values which are less than the mean values observed for the 60 000 gears tested. Five of them (gears 7, 8, 9, 33 and 34) show m_k and m_{ste} values which are less than the values observed for the standard gear. The others show a smaller value for m_k and a larger value for m_{ste} than the standard gear.

5.3 Results analysis and discussion

The multi-objective optimization performed leads to various solutions which provide great benefits in terms of design choice.

Indeed, two close points of the Pareto front (see figure 10) can have similar performance even if they correspond to very different sets of design parameters. For example, m_k value is about 10% and m_{ste} value is
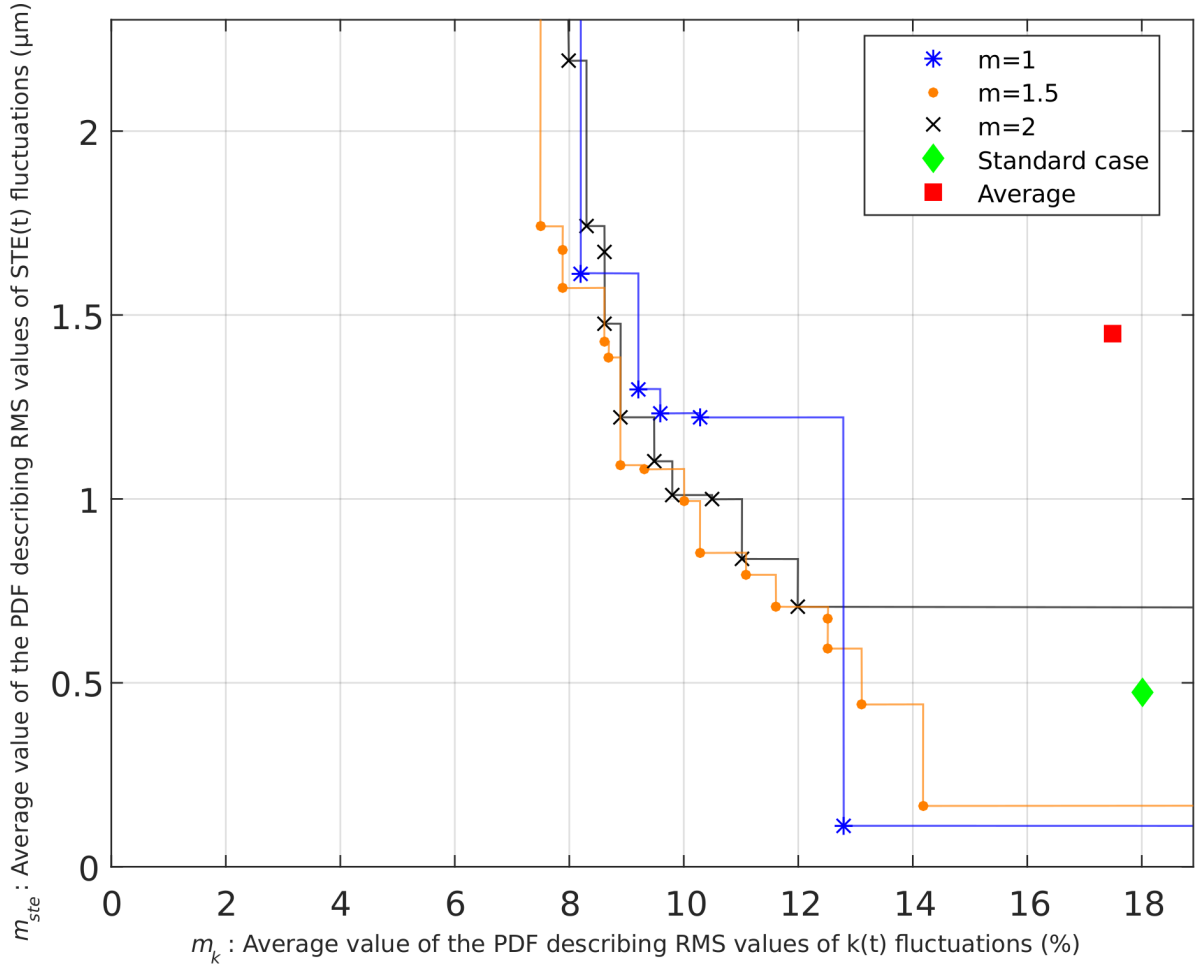
Fig. 8: *Pareto front of the optimization for the 3 gear cutting tools*

about 1 μm for both gears 22 and 47. However, gear 22 is characterized by a module equal to 1.5 mm, a number of teeth equal to 24 and a negative profile shift coefficient, whereas gear 47 is characterized by a module equal to 2 mm, a number of teeth equal to 17 and a positive profile shift coefficient. Another illustration corresponds to gears 10 and 11 built with the same gear cutting tool ($m = 1$). m_k value is about 7.7% and m_{ste} value is about 1.65 μm. However, gear 10 is characterized by a high positive profile shift coefficient and requires a longitudinal gear crowning whereas gear 11 is characterized by a negative profile shift and does not require any microgeometry modification.

From table 2, different gear categories can be identified that may orient the designer choice. All gears selected correspond to a number of teeth between $Z = 16$ and $Z = 37$. Regardless of mk and m_{ste} values, Z value may be a selection criterion because the main spectral components of the excitation source generated by the meshing process correspond to harmonics of the mesh frequency which is multiple of the teeth number. A modal analysis of the mechanical gear system allows identification of the critical modes which may be excited by the meshing process under operating conditions [56]. Such analysis permits to eliminate the gears likely to excite these critical modes, despite a minimized excitation amplitude.

Most of the gears selected in table 2 have a high helix angle β, a positive profile shift x_{ps} and do not require crowning corrections C_β. A high helix angle allows progressive entry of teeth into the contact area unlike spur gears. Few gears show a low helix angle (5°, namely gears 1, 10, 11, 12, 36 and 37), which minimizes
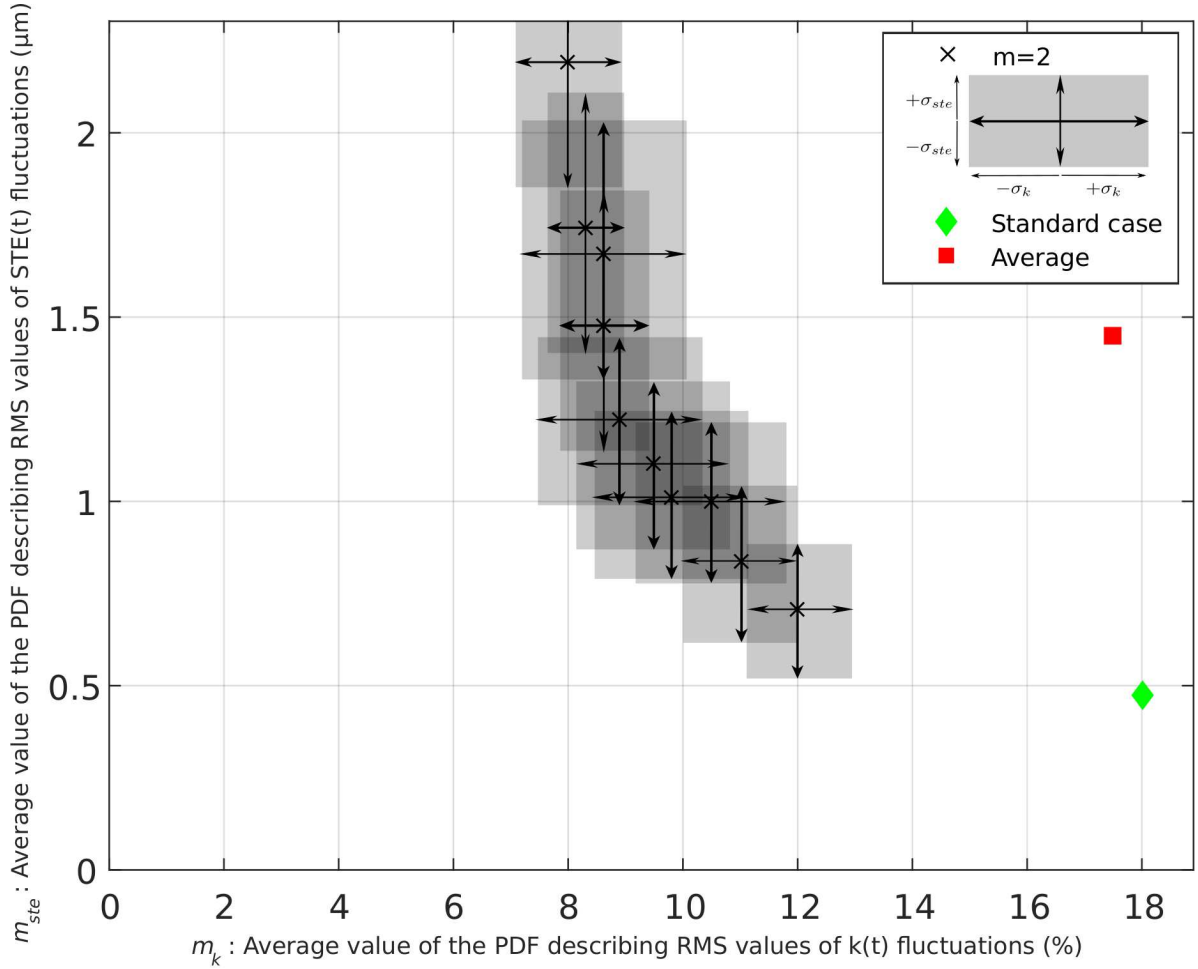
Fig. 9: *Pareto front of the gear cutting tool 3 ($m_3 = 2$ mm, $\alpha_3 = 20^o$) with an insight of the dispersion*

the risks caused by the axial load transmitted by the gear to the shafts, bearings and housing of the mechanical gear system. These gears usually show a small value for mk and a large value for m_{ste}.

One should also note that some gears present exotic macrogeometry parameters such as a high profile shift coefficient x_{ps} and truncated teeth corresponding to a low addendum coefficient h_a. However, one can opt for more conventional designs. Indeed, many gears show a low profile shift coefficient (with an absolute value under 0.15) and a standard tooth addendum coefficient higher than 0.8 (namely gears 7, 8, 9 for the first gear cutting tool and gears 29 to 35 for the second gear cutting tool). These gears usually show a large value for mk and a small value for m_{ste}.

Few gears do not require any micro-level corrections (namely gear 8, 11, 12, 34 and 37), which simplifies the

manufacturing process.

The robustness of the objectives to manufacturing errors can also be a criterion to help the designer choose the best solution. It can be analysed from the 4 last columns indicating the standard deviations (σ_k and σ_{ste}) and the maximum values (M_k and M_{ste}) of the PDF describing the RMS values of $k(t)$ and STE $\delta(t)$ fluctuations. The smaller σ_k (respectively σ_{ste}), the higher the probability of the real value to be close to the objective average value. The maximum value M_k (respectively M_{ste}) reflects the worst manufacturing error case regarding k(t) (respectively STE $\delta(t)$) obtained with the 1000 random samples. Therefore these values may also constitute an essential criterion of choice.

For example, gears 7 and 8 are both characterized by the smallest standard deviation σ_{ste} (0.05 μm) as well
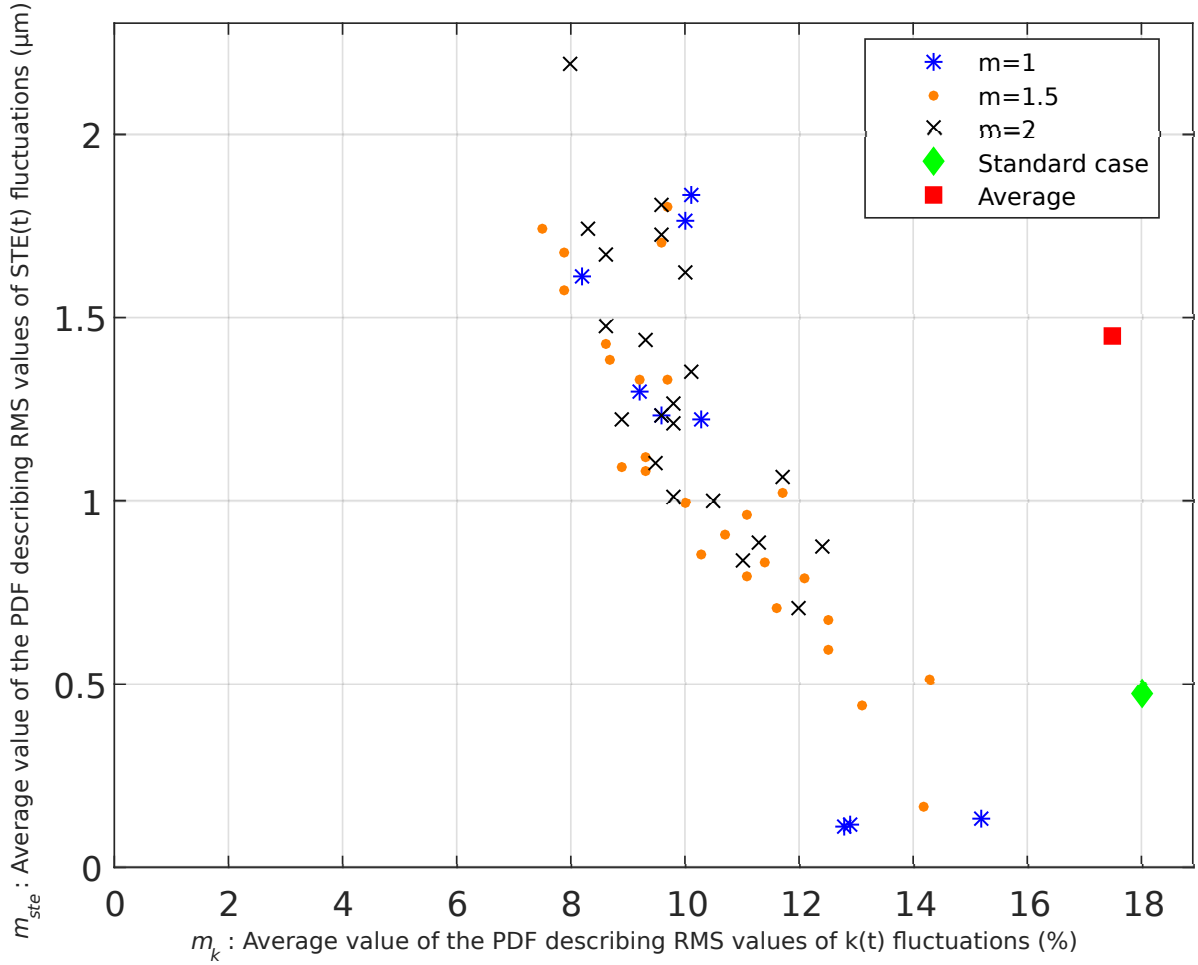
Fig. 10: *Wide Pareto front of the optimization for the 3 gear cutting tools*

as a small maximum value M_{ste} (0.27 and 0.29 μm), in addition to a particularly small mean value m_{ste} (0.11 and 0.12 μm), Consequently, these two gears appear to be very efficient and robust in term of low STE $\delta(t)$ excitation. Similarly, gear 39 is characterized by a small standard deviation σ_k (0.8%) as well as a small maximum value a small maximum value M_k (11%), in addition to a particularly small mean value mk (8.0%), This gear appears to be very efficient and robust in term of low k(t) excitation. On the contrary, gear 2 is characterized by a high standard deviation σ_k (1.6%) as well as a small maximum value a small maximum value M_k (16.8%), despite a particularly small mean value mk (9.2%).

More than a proper criterion, the standard deviations σ and the maximum values M of the objectives may be seen as a discriminant factor between two gears when all

the other criteria are taken into account, selecting one for its robustness or removing the other. One also may imagine some different optimization objectives that mix both the average value m, the standard deviation σ and the maximum value M of the PDF in order to select the best compromise between performance and robustness.

Finally, the methodology thus provides a decision help tool for the designer who intends to choose the best gear according to the problem encountered. For a mechanical gear system subjected to external force fluctuations such as input/output torques fluctuations, the coupling between these excitations and the parametric excitation associated with the mesh stiffness fluctuation provides an enrichment of the spectral content of the dynamic response as well as an increase of the global vi-

broacoustic level. In this case, minimization of the mesh stiffness fluctuation appears to be the most important objective [57]. For a mechanical gear system presenting some critical eigenmodes which may be excited by STE fluctuation under operating conditions, its minimization may be overriding compared to the minimization of the mesh stiffness fluctuation [56, 12].

6   Conclusion

In a NVH context, this paper introduces an original methodology for the multi-objective optimization of mechanical gear systems vibroacoustic behavior. Unlike most NVH gear optimizations, its objective functions are to minimize both the Static Transmission Error (STE) and the mesh stiffness $k(t)$ fluctuations. The other originality is to include both macro and microgeometry parameters. This methodology also takes into account the robustness of solutions to manufacturing errors through Monte Carlo simulations included in the optimization procedure.

The optimization is performed using a genetic algorithm NSGA-II with the advantage of exploring the global design space. It tests a high number of gears and make them evolve through generations in order to find the best compromises between the objectives. This type of algorithm involves repetitive calculations and requires an efficient model to evaluate gear excitation sources of each gear. For this reason, a semi-analytical tooth bending model is introduced. It is based on the modeling of the gear teeth compliance by a thick Reissner-Mindlin plate analytical model and a Ritz-Galerkin approximation of the tooth deflection form. This model is proven very efficient with a computational time about 1000 times shorter than a finite element model, for a relative error remaining under 10%.

The set of design parameters chosen for the optimization procedure corresponds to both macrogeometry parameters (gear tool module and pressure angle, number of teeth, helix angle and teeth addendum) and micro-

geometry parameters (crowning, amount and length of tip relief). Considering the variability induced by manufacturing tolerances, a Monte Carlo simulation is performed with a thousand samples of random manufacturing errors for each gear design tested by the algorithm. The Power Density Functions (PDF) describing the RMS values of $k(t)$ and STE $\delta(t)$ fluctuations are estimated for each gear, and its two objectives are the minimization of the average values of these PDF.

The methodology efficiency is demonstrated with an application example of a mechanical system equipped with a reverse gear. Three different gear cutting tools are used.
The algorithm tests more than 60 000 gears and selects a hundred of gears which correspond to the best compromises between the objectives. It provides a wide range of results which systematically minimize STE $\delta(t)$ and $k(t)$ fluctuation, compared to the initial standard spur gear.
The methodology then turns into a decision help tool for the designer who may choose the best gear regarding its problem. One may consider multiple criteria:

- The objectives values may favour a low $k(t)$ fluctuation or a low STE $\delta(t)$ excitation. The user must study the mechanical device he wants to improve and the operating conditions in order to identify the prominence of one excitation source compared to the other.
- The various solutions obtained can show very similar objectives values with very different gear designs. They provide great benefits for the choice of the best solution. One may select a gear in function of the manufacturing cost or the number of teeth and the corresponding meshing frequency.
- The dispersion of the PDF (standard deviations and maximum values) may characterize more specifically the robustness of each selected gear to the manufacturing errors and can also be seen as a discriminant or promoting criterion of choice.

Ongoing researches develop the perspective of includ-

ing both the average values and standard deviations as objective functions.

References

[1] Rémond, D., Velex, P., and Sabot, J., 1993. "Comportement dynamique et acoustique des transmissions par engrenages: synthèse bibliographique (dynamic and acoustic analysis of gear transmissions: bibliographic reviews)". Publication CETIM.

[2] Harris, S., 1958. "Dynamic loads on the teeth of spur gears". Proceedings of the Institution of Mechanical Engineers, **172**(1), pp. 87–112.

[3] Welbourn, D., 1979. Fundamental knowledge of gear noise: a survey. Tech. rep.

[4] Opitz, H., 1968. "Noise of gears". Philosophical Transactions of the Royal Society of London. Series A, Mathematical and Physical Sciences, **263**(1142), pp. 369–380.

[5] Carbonelli, A., Rigaud, E., and Perret-Liaudet, J., 2016. "Vibro-acoustic analysis of geared systems - predicting and controlling the whining noise". In Automotive NVH Technology. Springer, pp. 63–79.

[6] Rigaud, E., Sabot, J., and Perret-Liaudet, J., 2000. "Comprehensive approach for the vibrational response analysis of a gearbox". Revue européenne des éléments finis, **1-3**, pp. 315–330.

[7] Tavakoli, M., and Houser, D., 1986. "Optimum profile modifications for the minimization of static transmission errors of spur gears". Journal of Mechanisms, Transmissions, and Automation in Design, **108**(1), pp. 86–94.

[8] Rigaud, E., and Barday, D., 1999. "Modelling and analysis of static transmission error. effect of wheel body deformation and interactions between adjacent loaded teeth". In 4th world congress on gearing and power transmission, Paris, Vol. 3, pp. 1961–1972.

[9] Rigaud, E., and Barday, D., 1998. "Modélisation et analyse de l'erreur statique de transmission d'un engrenage. influence des déformations des roues et interactions entre les couples de dents en prise". Mécanique industrielle et matériaux, **51**, pp. 58–60.

[10] Umeyama, M., 1995. "Effects of deviation of tooth surface errors of a helical gear pair on the transmission error". Nippon Kikai Gakkai Ronbunshu, C Hen/Transactions of the Japan Society of Mechanical Engineers, Part C, **61**(587), pp. 3101–3107.

[11] Kurokawa, S., Ariura, Y., and Ohtahara, M., 1996. "Transmission errors of cylindrical gears under load-influence of tooth profile modification and tooth deflection". American Society of Mechanical Engineers, Design Engineering Division (Publication) DE, **88**, pp. 213–217.

[12] Rigaud, E., Sabot, J., and Perret-Liaudet, J., 1999. "Effect of gearbox design parameters on the vibratory response of its housing". In 4th World Congress on Gearing and Power Transmission, Paris, Vol. 3, pp. 2143–2148.

[13] Kapelevich, A., and Kleiss, R., 2002. "Direct gear design for spur and helical involute gears.". Gear Technology, **19**(5), pp. 29–35.

[14] Wink, C., and Serpa, A., 2005. "Investigation of tooth contact deviations from the plane of action and their effects on gear transmission error". Proceedings of the Institution of Mechanical Engineers, Part C: Journal of Mechanical Engineering Science, **219**(5), pp. 501–

509.

[15] Houser, D., and Harianto, J., 2005. The effect of micro-geometry and load on helical gear noise excitations. Tech. rep., SAE Technical Paper.

[16] Driot, N., and Perret-Liaudet, J., 2006. "Variability of modal behavior in terms of critical speeds of a gear pair due to manufacturing errors and shaft misalignments". Journal of Sound and Vibration, **292**(3), pp. 824–843.

[17] Chang, S., Houser, D., and Harianto, J., 2003. "Tooth flank corrections of wide face width helical gears that account for shaft deflections". In ASME 2003 International Design Engineering Technical Conferences and Computers and Information in Engineering Conference, American Society of Mechanical Engineers, pp. 567–574.

[18] Kahraman, A., Bajpai, P., and Anderson, N., 2005. "Influence of tooth profile deviations on helical gear wear". Journal of Mechanical Design, **127**(4), pp. 656–663.

[19] Guilbault, R., Gosselin, C., and Cloutier, L., 2006. "Helical gears, effects of tooth deviations and tooth modifications on load sharing and fillet stresses". Journal of Mechanical Design, **128**(2), pp. 444–456.

[20] Bruyère, J., and Velex, P., 2013. "Derivation of optimum profile modifications in narrow-faced spur and helical gears using a perturbation method". Journal of Mechanical Design, **135**(7), p. 071009.

[21] Vedmar, L., 1981. On the design of external involute helical gears. na.

[22] Harianto, J., and Houser, D., 2007. "A methodology for obtaining optimum gear tooth micro-topographies for noise and stress minimization over a broad operating torque range". In ASME 2007 International Design Engineering Technical Conferences and Computers and Information in Engineering Conference, American Society of Mechanical Engineers, pp. 289–303.

[23] Driot, N., Rigaud, E., Sabot, J., and Perret-Liaudet, J., 2001. "Allocation of gear tolerances to minimize gearbox noise variability". Acta Acustica

united with Acustica, **87**(1), pp. 67–76.

[24] Vanderplaats, G., Chen, X., and Zhang, N.-T., 1988. Gear optimization. Tech. rep., NASA.

[25] Kapelevich, A., and Shekhtman, Y., 2003. "Direct gear design: Bending stress minimization.". Gear technology, **20**(5), pp. 44–47.

[26] Savsani, V., Rao, R., and Vakharia, D., 2010. "Optimal weight design of a gear train using particle swarm optimization and simulated annealing algorithms". Mechanism and machine theory, **45**(3), pp. 531–541.

[27] Mohan, Y. M., and Seshaiah, T., 2012. "Spur gear optimization by using genetic algorithm". International Journal of Engineering Research and Applications, **2**(1), pp. 311–318.

[28] Singh, A., Gangwar, H., Saxena, R., and Misra, A., 2012. "Optimization of internal spur gear design using genetic algorithm". MIT International Journal of Mechanical Engineering, **2**(1), pp. 22–30.

[29] Munro, R., Yildirim, N., and Hall, D., 1990. "Optimum profile relief and transmission error in spur gears". Gearbox noise and vibration, pp. 35–42.

[30] Beghini, M., Presicce, F., and Santus, C., 2004. A method to define profile modification of spur gear and minimize the transmission error. AGMA.

[31] Eritenel, T., and Parker, R., 2005. "A static and dynamic model for three-dimensional, multi-mesh gear systems". In ASME 2005 International design engineering technical conferences and computers and information in engineering conference, American Society of Mechanical Engineers, pp. 945–956.

[32] Kang, J. S., and Choi, Y.-S., 2008. "Optimization of helix angle for helical gear system". Journal of mechanical science and technology, **22**(12), pp. 2393–2402.

[33] Akerblom, M., 2008. Gear geometry for reduced and robust transmission error and gearbox noise. Tech. rep., Volvo CE Component Division.

[34] Carbonelli, A., Perret-Liaudet, J., Rigaud, E., and Le Bot, A., 2011. "Particle swarm optimization as an efficient computational method in order to min-

imize vibrations of multimesh gears transmission". Advances in Acoustics and Vibration, **2011**.

[35] Bonori, G., Barbieri, M., and Pellicano, F., 2008. "Optimum profile modifications of spur gears by means of genetic algorithms". Journal of sound and vibration, **313**(3), pp. 603–616.

[36] Ghribi, D., Bruyère, J., Velex, P., Octrue, M., and Haddar, M., 2012. "Robust optimization of gear tooth modifications using a genetic algorithm". In Condition Monitoring of Machinery in Non-Stationary Operations. Springer, pp. 589–597.

[37] Bruyère, J., Gu, X., and Velex, P., 2015. "On the analytical definition of profile modifications minimising transmission error variations in narrow-faced spur helical gears". Mechanism and machine theory, **92**, pp. 257–272.

[38] Chapron, M., Velex, P., Bruyère, J., and Becquerelle, S., 2016. "Optimization of profile modifications with regard to dynamic tooth loads in single and double-helical planetary gears with flexible ring-gears". Journal of Mechanical Design, **138**(2), p. 023301.

[39] Lagaros, N., and Papadopoulos, V., 2006. "Optimum design of shell structures with random geometric, material and thickness imperfections". International Journal of Solids and Structures, **43**, pp. 6948–6964.

[40] Araujo, A., Martins, P., Mota Soares, C., C.A., M. S., and Herskovits, J., 2009. "Damping optimization of viscoelastic laminated sandwich composite structures". Structural and Multidisciplinary Optimization, **39**, pp. 569–579.

[41] Paluch, B., Grédiac, M., and Faye, A., 2008. "Combining a finite element programme and a genetic algorithm to optimize composite structures with variable thickness". Composite and Structures, **83**, pp. 284–294.

[42] Kudikala, R., Deb, K., and Bhattacharya, B., 2009. "Multi-objective optimization of piezoelectric actuator placement for shape control of plates using genetic algorithms". Journal of Mechanical Design, **131**, pp. 091007–1–11.

[43] Groşan, C., and Dumitrescu, D., 2002. "A comparison of multiobjective evolutionary algorithms". Acta Universitatis Apulensis, **4**.

[44] Zitzler, E., and Thiele, L., 1999. "Multiobjective evolutionary algorithms: a comparative case study and the strength pareto approach. evolutionary computation". IEEE transactions on Evolutionary Computation, **3(4)**, pp. 257–271.

[45] Zitzler, E., Deb, K., and Thiele, L., 1999. Comparison of multiobjectivr evolutionary algorithms: empirical results. Tech. rep., Technical Report 70, Computer Engineering and Networks Laboratory (TIK), Swiss Federal Institute of Technology (ETH) Zurich.

[46] Zitzler, E., Laumanns, E., and Thiele, L., 2001. Spea2: Improving the strength pareto evolutionary algorithm. Tech. rep., Technical Report 103, Computer Engineering and Networks Laboratory (TIK), Swiss Federal Institute of Technology (ETH) Zurich.

[47] Srinivas, N., and Deb, K., 1994. "Multiobjective optimization using nondominated sorting in genetic algorithms". Journal of Evolutionary Computation, **2**, pp. 221–248.

[48] Deb, K., Agrawal, S., Pratap, A., and Meyarivan, T., 2000. "A fast elitist non-dominated sorting genetic algorithm for multi-objective optimization: Nsga-2". Notes in Computer Science.

[49] Deb, K., Pratap, A., Agrawal, S., and Meyarivan, T., 2002. "A fast and elitist multiobjective genetic algorithm: Nsga-2". Transactions on evolutionary computation, **6 (2)**.

[50] Knowles, J., and Corne, D., 1999. "The pareto archived evolution strategy: A new baseline algorithm for pareto multiobjective optimization". Congress on Evolutionary Computation (CEC 99), **1, Piscataway**, pp. 98–105.

[51] Dumitrescu, D., Groşan, C., and Oltean, M., 2001. "Simple multiobjective evolutionary algorithm". In Seminars on Computer Science, Faculty of Math-

ematics and Computer Science, Babeş-Boylai University of Cluj-Napoca.

[52] Dumitrescu, D., Groşan, C., and Oltean, M., 2001. "A new evolutionary adaptative representation paradigm". Studia Universitas Babes-Boylai, Seria Informatica, **XLVI(1)**, pp. 15–30.

[53] Reissner, E., 1945. "The effect of transverse shear deformation on the bending of elastic plates". Journal of Applied Mechanics, **12**, pp. 69–76.

[54] Reissner, E., 1950. "On a variational theorem in elasticity". Journal of Mathematics and Physics, **29**, pp. 90–95.

[55] Rigaud, E., 1998. "Interactions dynamiques entre denture, lignes d'arbres, roulements et carter dans les transmissions par engrenages (dynamic interactions between teeth, shaft lines, bearings, and housing in gear transmissions)". PhD thesis, Ecole Centrale de Lyon.

[56] Rigaud, E., and Sabot, J., 1996. "Effect of elasticity of shafts, bearings, casing and couplings on the critical rotational speeds of a gearbox". VDI Berichte, **1230**, pp. 833–845.

[57] Garambois, P., Donnard, G., Rigaud, E., and Perret-Liaudet, J., 2017 / To be published. "Multiphysics coupling between periodic gear mesh excitation and input/output fluctuating torques: application to a roots vacuum pump". Journal of Sound and Vibration.